



1 On the relevance of extremal dependence for spatial
2 statistical modelling of natural hazards

3 Laura C. Dawkins^{1*} and David B. Stephenson¹

¹ College of Engineering, Mathematics and Physical Sciences, University of Exeter,
Exeter, UK

* E-mail: L.C.Dawkins@exeter.ac.uk



4

Abstract

5

Natural hazard loss portfolios with exposure over a region are sensitive to the dependency between extreme values of the key hazard variable at different spatial locations. It is therefore important to correctly identify and quantify dependency to avoid poor quantification of risk.

6

7

8

9

This study demonstrates how bivariate extreme value tail dependency methods can be used together in a novel way to explore and quantify extremal dependency in spatial hazard fields. A relationship between dependency and loss is obtained by deriving how the probability distribution of conceptual loss depends on the tail dependency coefficient.

10

11

12

13

14

The approaches are illustrated by applying them to 6103 historical European windstorm footprints (spatial maps of 3-day maximum gust speeds). We find there is little evidence of asymptotic extremal dependency in windstorm footprints. Furthermore, empirical extremal properties and conceptual loss distributions between pairs of locations are shown to be well reproduced using Gaussian copulas but not by extremally-dependent models such as Gumbel copulas.

15

16

17

18

19

20

It is conjectured that the lack of asymptotic dependence is a generic property of turbulent flows, which may extend to other spatially continuous hazards such as heat waves and air pollution. These results motivate the potential of using Gaussian process (geostatistical) models for efficient simulation of hazard fields.

21

22

23

24

Key Words: Natural hazards; Windstorm footprint; Bivariate dependence; Reinsur-

25

ance; Copulas



26 **1 Introduction**

27 Multivariate statistical models are increasingly used to explore the spatial characteris-
28 tics of natural hazards and quantify potential risk. For example, multivariate statistical
29 models for European windstorms are used by academics and re/insurers to create cata-
30 logues of possible events, explore loss potentials, and benchmark synthetic events from
31 atmospheric models (Bonazzi et al. 2012; Youngman and Stephenson 2016). Since nat-
32 ural hazards are rare events in the tail of the distribution, correctly modelling extremal
33 dependence is very important for valid inference (Eastoe et al., 2013), which, in turn, is
34 essential for realistically representing potential hazard losses, often occurring at multiple
35 spatial locations.

36 As noted by Wadsworth et al. (2017), examples of modelling joint extremes often
37 assume asymptotic dependence in order to accommodate asymptotically justified extreme
38 value max-stable models. This is also common in the field of natural hazard research.
39 Coles and Walshaw (1994) used a max-stable model for the dependence in maximum
40 wind speeds in different directions; Blanchet et al. (2009) to model snow fall in the Swiss
41 Alps; Huser and Davison (2013) to model extreme rainfall and Bonazzi et al. (2012) to
42 model windstorm hazard fields at pairs of locations in Europe. Indeed, Bonazzi et al.
43 (2012) simply base this modelling assumption on being “in line with many examples found
44 in the literature”. Therefore, it seems sensible to ask, how valid is this assumption of
45 asymptotic dependence? And how much of an effect might a misspecification of extremal
46 dependence have on the resulting hazard loss representation?

47 Contrary to the above examples, Bortot et al. (2000) provided a brief exploration
48 of the extremal dependence between measurements of sea surge, wave height and wave
49 period recorded off the south-west coast of England. Using pairwise scatter plots and



50 empirical estimates of the Extremal Dependence coefficients, χ and $\bar{\chi}$, introduced by
51 Coles et al. (1999), they found evidence for asymptotic independence, and hence devel-
52 oped a multivariate Gaussian tail model for their data, derived from the joint tail of a
53 multivariate Gaussian distribution with margins based on univariate extreme value distri-
54 butions. Bortot et al. (2000) showed that, when modelling data that are asymptotically
55 independent, the Gaussian model is robust, has simple diagnostics, easily interpretable
56 parameters and extends straightforwardly to higher dimensions. Similarly, Youngman
57 and Stephenson (2016) acknowledged the possibility of asymptotic independence when
58 developing a spatial statistical framework for simulating natural hazard events. They
59 specified a Student's t-process to model dependence, allowing for the form of extremal
60 dependence to be determined by the estimated degrees of freedom parameter.

61 In this study, we provide a more rigorous, critical approach for investigating spatial
62 extremal dependence, which combines various bivariate extreme value modelling methods
63 in a novel way. We apply this approach to windstorm hazard fields to explore the validity
64 of the asymptotic dependence assumption made in previous studies, and provide a tur-
65 bulence argument for the form of extremal dependence found. Furthermore, we present
66 a comparison approach for exploring the impact of mis-specifying extremal dependence
67 on realistically representing conceptual windstorm losses.

68 To critically investigate spatial extremal dependence we initially employ the Extremal
69 Dependence coefficients of Coles et al. (1999), $\chi(p)$ and $\bar{\chi}(p)$, characterising the condi-
70 tional probability of a pair of locations exceeding the same high quantile threshold, $1 - p$.
71 The upper limit of these dependence measures determines the class of extremal depen-
72 dence, hence this limit is explored both empirically, as in Bortot et al. (2000), and based
73 on a number of parametric representations. For a given pair of locations within a wind-



74 storm hazard field, we fit Gumbel and Gaussian bivariate copula dependence models, each
75 characterising opposing extremal dependence class, and explore how well these models
76 represent the empirical estimates of $\chi(p)$ and $\bar{\chi}(p)$. In addition, we fit the bivariate tail
77 model of Ledford and Tawn (1996), able to characterise both classes of extremal de-
78 pendence, and use the extremal dependence diagnostic approach of Ledford and Tawn
79 (1996, 1997) to further identify extremal dependence class based on the coefficient of tail
80 dependence parameter of this model.

81 The impact of extremal dependence mis-specification on conceptual loss estimation is
82 explored by comparing how well the Gumbel and Gaussian copula dependence models are
83 able to represent empirical conceptual joint loss. Based on existing literature in the field
84 of windstorm modelling, a quantile threshold exceedance loss model is proposed. The
85 copula model comparison is then made in terms of their ability to represent $\chi(p)$ and
86 $\bar{\chi}(p)$ for the specified conceptual loss quantile threshold, and the expected conditional
87 conceptual joint loss distributions for pairs of locations throughout Europe.

88 In applying a similar critical investigation to an alternative continuous spatial variable,
89 such as temperature, relevant for modelling heat wave risk, a natural hazard modeller
90 will be able to diagnose the extremal dependence class present in the spatial field and
91 explore the sensitivity of conceptual loss to a misspecification of this class. Rather than
92 fitting a more complex model that can accommodate both types of extremal dependence,
93 and therefore requires the estimation of additional parameters, this diagnostic approach
94 allows the modeller to develop a model that specifically represents this statistical property,
95 and hence the loss potentials, correctly; either using a max-stable model to characterise
96 asymptotic dependence, as is most common in examples in the literature, or a Gaussian,
97 or geostatistical model to characterise asymptotic independence, shown by Bortot et al.



98 (2000) to be robust and accurate in the upper tail.

99 The remaining paper is organised as follows. The windstorm hazard data set, used
100 throughout this paper, is described in Section 2. Our novel approach for critically inves-
101 tigating spatial extremal dependence is presented and applied to the windstorm hazard
102 data in Section 3, including a physical explanation for the form of extremal dependence
103 identified, in Section 3.4. Section 4 describes our novel method for exploring the impact
104 of extremal dependence on conceptual loss estimation, again applied to the windstorm
105 data set.

106 2 Data

107 The windstorm footprint data set used in this paper is the same as that used in Dawkins
108 et al. (2016), consisting of the 6103 windstorm events that occurred within the European
109 domain during the 35 extended winters, October - March 1979/80 - 2013/14 (kindly
110 provided by J. Standen and J. F. Lockwood at the Met Office).

111 The windstorm footprint is defined as the maximum three second wind gust speed
112 (in ms^{-1}) at grid points in the region 15°W to 25°E in longitude and 35°N to 70°N in
113 latitude over a 72 hour period centred on the time at which the maximum 925hPa wind
114 speed occurred over land. The 925hPa wind speed is taken from ERA-interim reanalysis
115 (Dee et al., 2011). The three second wind gust speed has a robust relationship with storm
116 damage (Klawns and Ulbrich, 2003), and is commonly used in catastrophe models for risk
117 quantification (Roberts et al., 2014). A 72 hour windstorm duration is commonly used
118 in the insurance industry (Haylock, 2011), and is thought to capture the most damaging
119 phase of the windstorms (Roberts et al., 2014).

120 These 6103 historical windstorm events have been identified using the objective track-



121 ing approach of Hodges (1995) and the associated footprints are created by dynamically
122 downscaling ERA-Interim reanalysis to a horizontal resolution of 25km using the Met
123 Office unified model (MetUM). The wind gust speeds are calculated from wind speeds in
124 the MetUM model, based on a simple gust parameterisation $U_{gust} = U_{10m} + C\sigma$, where
125 U_{10m} is the wind speed at 10 metre altitude, C is a constant determined from the universal
126 turbulence spectra and σ is the standard deviation of the horizontal wind.

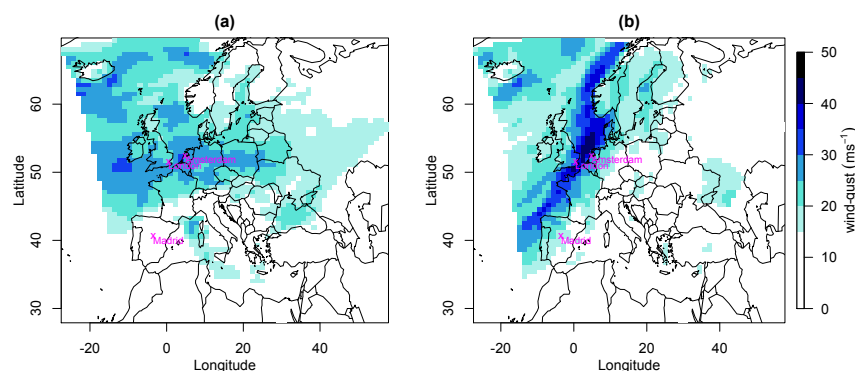


Figure 1: Hazard footprints for windstorms (a) Kyrill and (b) the Great Storm of October '87, with the location of the cities of London, Amsterdam and Madrid indicated.

127 Two such footprints for windstorms Kyrill (17th – 19th January 2007) and the Great
128 Storm of October '87 (15th – 17th October 1987) are shown in Fig. 1. The variability in
129 the intensity and location of extreme, damaging winds in these footprints demonstrate
130 the potential importance of correctly modelling the spatial dependence between locations
131 for realistically representing joint losses.



132 **3 Extremal Dependency**

133 We show how various bivariate extreme value modelling methods can be brought together
134 in a novel way to critically investigate the bivariate extremal dependence property of
135 windstorm hazard fields. This approach is illustrated based windstorm footprint wind
136 gust speeds at two pairs of locations, London-Amsterdam and London-Madrid. These
137 three locations are shown in Fig. 1, and these two pairings are chosen because of their
138 contrasting separation distances and directions, and hence degrees of dependence.

139 **3.1 Graphical summary using the empirical copula**

140 As a motivating example, the bivariate dependence in windstorm footprint wind gust
141 speeds for London paired with Amsterdam and Madrid are presented in Figures 2 (a)
142 and (c) respectively. These scatter plots show a greater degree of dependence between
143 London and Amsterdam compared to London and Madrid. Indeed, multiple windstorms
144 have losses occurring in London and Amsterdam at the same time, when loss is associated
145 with wind gust speeds exceeding the 99% quantile at a given location, characterised by
146 the top right-hand corner of each plot in Fig. 2. However, does this level of dependence
147 between London and Amsterdam necessarily suggest asymptotic dependence?

148 Let the $n \times 2$ variable (X, Y) represent the wind gust speeds associated with the
149 $n = 6103$ windstorm events at any given pair of locations within the European domain,
150 e.g. London and Amsterdam. The bivariate relationship between X and Y can be
151 represented by two components, the marginal distributions of each variable, and their
152 joint dependence. The dependence component of the relationships shown in Fig. 2 (a)
153 and (c) can therefore be isolated by, for each location, transforming wind gust speeds
154 associated with each of the windstorm events, e.g. X_i for $i = 1, \dots, n$, to uniform margins

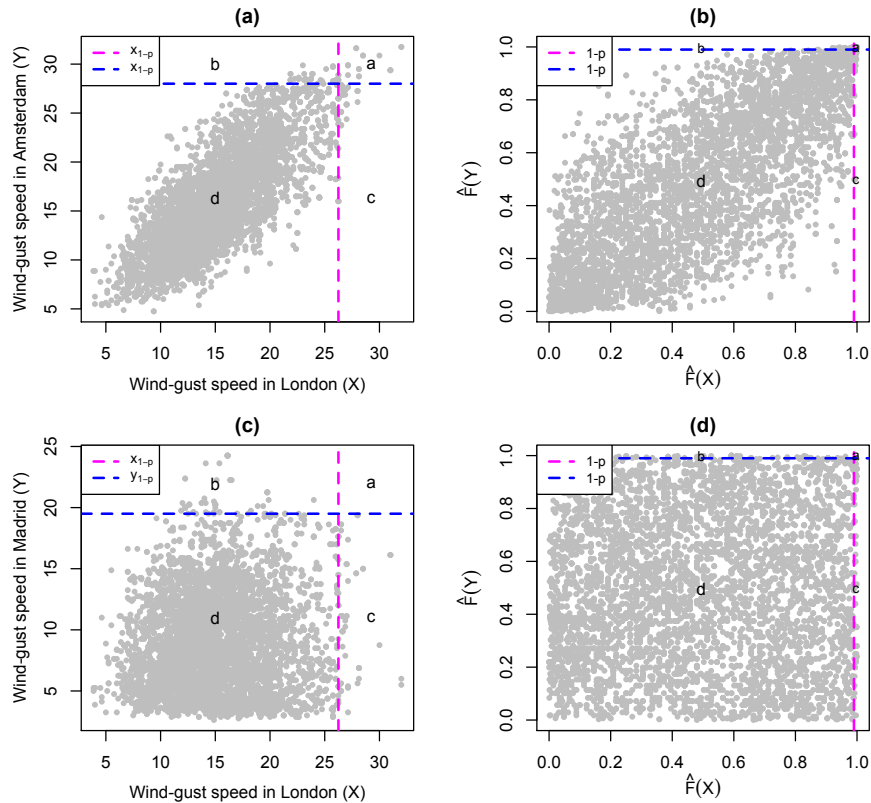


Figure 2: Scatter plot/empirical copulas comparing historical windstorm footprint wind gust speeds (ms^{-1}) in London paired with (a)/(b) Amsterdam and (c)/(d) Madrid. Dashed lines show the 99% quantile of wind gust speed at each location, and labels a-d represent the number of points in each section of each plot, related to being above or below these high quantile thresholds.

155 using the estimator of the empirical distribution function ($\frac{1}{n} \sum_{j=1}^n \mathbf{1}_{X_j \leq x_i}$), shown in Fig.

156 2 (b) and (d) respectively. This is known as the empirical copula.



157 3.2 Measures for quantifying extremal dependence

158 The degree of conditional dependence between locations, at a specified high quantile
159 threshold, $1 - p$, can then be explored, based on the empirical copula, using the Ex-
160 tremal Dependence Coefficients, $\chi(p)$ and $\bar{\chi}(p)$, introduced by Coles et al. (1999), and
161 the asymptotic limit of these measures, as $p \rightarrow 0$, classifies the class of bivariate extremal
162 dependence as either *asymptotically dependent* or *asymptotically independent*. These mea-
163 sures are defined as,

$$\chi(p) = \Pr(Y > y_{1-p} | X > x_{1-p}) = \frac{\Pr(Y > y_{1-p}, X > x_{1-p})}{p}, \quad (1)$$

164 where x_{1-p} and y_{1-p} are the $(1 - p)^{th}$ quantiles of X and Y respectively, $0 \leq \chi(p) < 1$
165 for all $0 \leq (1 - p) \leq 1$, and,

$$\bar{\chi}(p) = \frac{2\log(\Pr(X > x_{1-p}))}{\log(\Pr(X > x_{1-p}, Y > y_{1-p}))} - 1 = \frac{2\log(p)}{\log(\chi(p)p)} - 1 = \frac{\log(p) - \log(\chi(p))}{\log(p) + \log(\chi(p))}, \quad (2)$$

166 where $-1 \leq \bar{\chi}(p) < 1$ for all $0 \leq (1 - p) \leq 1$.

167 Hence, if $\lim_{p \rightarrow 0} \chi(p) = \chi(0) > 0$, $\lim_{p \rightarrow 0} \bar{\chi}(p) = \bar{\chi}(0) = 1$, and the pair (X, Y) are
168 said to be asymptotically dependent with strength $\chi(0)$. If instead $\chi(0) = 0$, and hence,
169 $\bar{\chi}(0) < 1$, the pair are said to be asymptotically independent, and the non-vanishing
170 measure $\bar{\chi}(0)$ represents the strength of this non-asymptotic dependence.

171 As an initial empirical exploration of bivariate extremal dependence class between
172 variables, these conditional probability measures can be calculated empirically over a
173 range of quantile thresholds, as shown in Fig. 3 for windstorm footprint wind gust speeds
174 in London paired with Amsterdam and Madrid. These empirical estimates are calculated
175 as functions of the counts (a,b,c,d) in Fig. 2, as defined in Table 1. Based on these em-

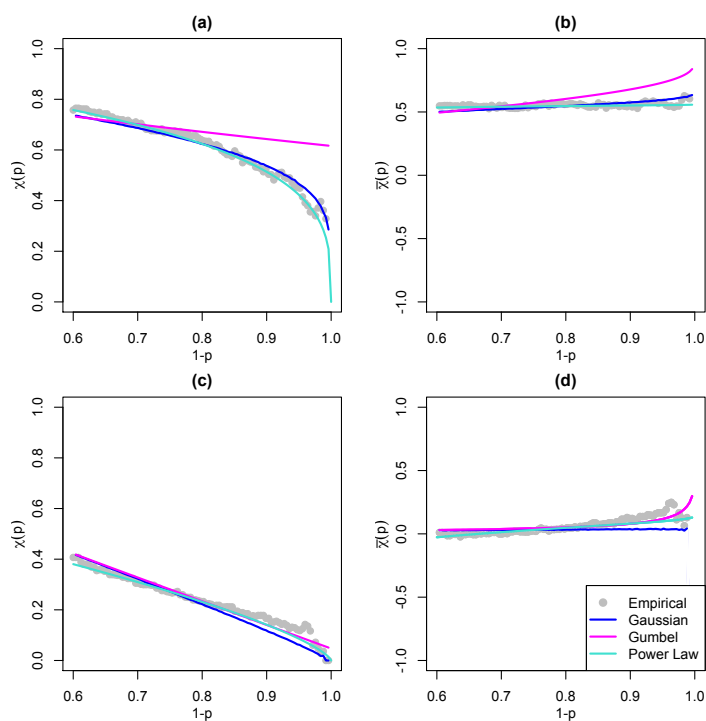


Figure 3: Dependence measures, $\chi(p)/\bar{\chi}(p)$, for $p \in [0, 0.4]$, for windstorm footprint wind gust speeds in London paired with (a)/(b) Amsterdam and (c)/(d) Madrid, calculated empirically and based on the Gaussian, Gumbel and Power Law bivariate dependence functions, as defined in Table 1.



176 pirical estimates, for both pairs of locations, $\chi(p) \rightarrow 0$ and $\bar{\chi}(p) < 1$ as $p \rightarrow 0$, suggesting
177 asymptotic independence. In addition, Fig. 3 presents three parametric representations
178 of these conditional probability measures, used to better explore the asymptotic limits,
179 $\chi(0)$ and $\bar{\chi}(0)$. These parametric forms are also shown in Table 1 and are discussed
180 further in Section 3.3.

181 **3.3 Estimation of the tail dependence coefficient**

182 The rarity of extreme events within this historical data set makes it impossible to empir-
183 ically quantify the asymptotic limits $\chi(0)$ and $\bar{\chi}(0)$, necessary for extremal dependence
184 class identification. To overcome this, Ledford and Tawn (1996) developed a bivariate
185 tail model, able to characterise both classes of extremal dependence, which when fit to a
186 bivariate random variable can be used to model the asymptotic limit of the conditional
187 probability measures and specify the class of extremal dependence.

188 As in Ledford and Tawn (1996), let Z_1 and Z_2 denote X and Y transformed to unit
189 Fréchet margins respectively, that is $\Pr(Z_1 \leq z) = \Pr(Z_2 \leq z) = \exp(-1/z)$. Then the
190 joint survivor function for Z_1 and Z_2 , above some large quantile threshold z_{1-p} , takes the
191 form,

$$\Pr(Z_1 > z_{1-p}, Z_2 > z_{1-p}) \sim \mathcal{L}(z_{1-p})p^{1/\eta}, \quad (3)$$

192 where $p = \Pr(Z_1 > z_{1-p}) = \Pr(Z_2 > z_{1-p})$, $\frac{1}{2} \leq \eta \leq 1$ is a constant and $\mathcal{L}(z_{1-p})$ is a
193 slowly varying function as $p \rightarrow 0$. Based on this power law model, as shown by Coles
194 et al. (1999),



$$\begin{aligned}\chi(p) &\sim \mathcal{L}(z_{1-p})p^{1/\eta-1}, \\ \bar{\chi}(p) &= \frac{2\log(p)}{\log(\mathcal{L}(z_{1-p})) + \frac{1}{\eta}\log(p)} - 1, \\ &\rightarrow 2\eta - 1 \quad \text{as } p \rightarrow 0.\end{aligned}$$

195 Hence, the parameter η , named the coefficient of tail dependence by Ledford and
196 Tawn (1996), characterises the nature of the asymptotic dependence. When $\eta = 1$,
197 $\chi(0) = \mathcal{L}(z_{1-p})$ and $\bar{\chi}(0) = 1$, hence the pair (X, Y) are asymptotically dependent of
198 degree $\mathcal{L}(z_{1-p})$. Alternatively, if $\eta < 1$, $\chi(0) = 0$ and $\bar{\chi}(0) = 2\eta - 1$, and the pair are
199 asymptotically independent with non-asymptotic dependence of degree $2\eta - 1$.

200 For a given pair, e.g. wind gust speeds in London and Amsterdam, the Ledford and
201 Tawn (1996) is fit to the joint survivor function along the diagonal, equivalent to the
202 univariate distribution of $T = \min\{Z_1, Z_2\}$, known as the structure variable, which has
203 length n . Using the stable two parameter Poisson process representation of T , presented
204 by Ferro (2007), who employed the Ledford and Tawn (1996) model for the verification
205 of extreme weather forecasts, the exceedance of T above a high threshold w has the form,

$$\Pr(T > t) = \frac{1}{n} \exp \left[- \left(\frac{t - \alpha}{\eta} \right) \right] \quad \text{for all } t \geq w, \quad (4)$$

206 with location parameter α and scale parameter $0 < \eta \leq 1$, equivalent to η in Eqn. (3),
207 estimated by maximum likelihood (Ferro, 2007).

208 We fit this model to the pairs London-Amsterdam and London-Madrid, requiring the
209 specification of the high threshold, w . This threshold must be high enough that this
210 asymptotic model is valid, but low enough that enough data are used to estimate the
211 parameters. Here, the 85% quantile of the structural variable T is selected, based on



212 stability plots of quantile thresholds w against model parameter estimates obtained by
213 fitting the model to exceedances of w . Based on this choice of w , $\eta = 0.78 < 1$ for London-
214 Amsterdam and $\eta = 0.58 < 1$ for London-Madrid, indicating asymptotic independence for
215 both pairs of locations. Figure 3 shows how these fitted models represent the asymptotic
216 limit of the conditional dependence measures $\chi(p)$ and $\bar{\chi}(p)$ as $p \rightarrow 0$, the Poisson process
217 form of which are presented in Table 1, referred to as the Power Law model.

218 In addition, alternative parametric bivariate dependence models, known as the Gaus-
219 sian and Gumbel copulas, characterising opposing extremal dependence class, can be used
220 to model the pair (X, Y) , and hence $\chi(p)$ and $\bar{\chi}(p)$, for comparison, also shown in Fig. 3.
221 The representation of $\chi(p)$ and $\bar{\chi}(p)$ in the limit $p \rightarrow 0$ for these opposing models then
222 gives further indication of the extremal dependence class.

223 The Gumbel bivariate copula model characterises asymptotic dependence with the
224 degree of dependence quantified by parameter r . For each pair of locations, this parameter
225 is estimated via maximum likelihood using the `copula` R package. The Gaussian bivariate
226 model characterises asymptotic independence with dependence parameter ρ , here, for
227 each pair of locations, represented by the Spearman's rank correlation coefficient. The
228 parametric forms of $\chi(p)$ and $\bar{\chi}(p)$ for these two opposing models are shown in Table 1.
229 In Fig. 3, the Gumbel model is calculated as in Table 1, however, since the closed form
230 definition for the Gaussian model in Table 1 only holds for the limit $p \rightarrow 0$, for this model
231 $\chi(p)$ and $\bar{\chi}(p)$ are estimated as the median of 1000 parametric bootstrap simulations from
232 the associated bivariate normal distribution.

233 For both pairs of locations in Fig. 3, the Power Law model characterises asymptotic
234 independence, since $\chi(0) = 0$ and $\bar{\chi}(0) < 1$. Asymptotic independence is further sup-
235 ported by the success of the Gaussian, and failure of the Gumbel, dependence models in

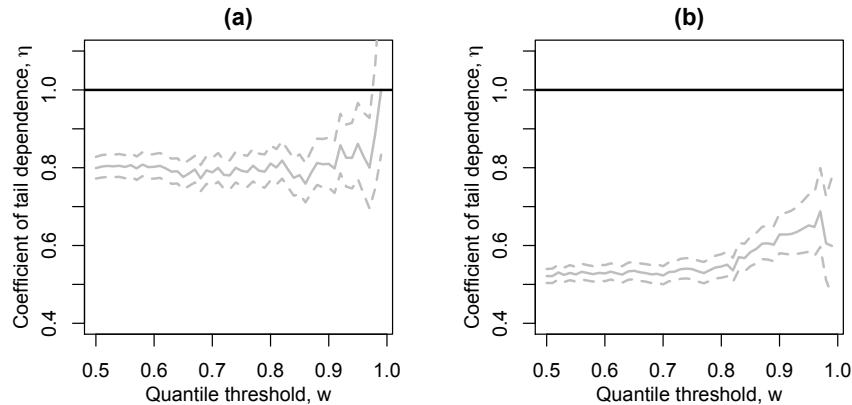


Figure 4: Diagnostic plots of maximum likelihood estimates (solid) and 95% profile likelihood confidence intervals (dashed) of η , in Eqn. (4), for threshold w in the range of the 0.5 – 1 quantile of T , for London paired with (a) Amsterdam and (b) Madrid.

236 capturing the empirical bivariate dependence structure in the upper limit, $p \rightarrow 0$. The
237 Gumbel model overestimates the conditional probability of joint extremes due to a mis-
238 specification of asymptotic dependence, while the Gaussian model matches closely with
239 the empirical estimates and the Power Law model.

240 The Power Law model shown in Fig. 3 is based on using a high threshold, w , equal
241 to the 85% quantile of the structural variable T . The resulting estimate of η , and hence
242 the identification of extremal dependence class, depends on this threshold choice, hence
243 the sensitivity of this diagnosis to the choice of threshold must be explored before a
244 conclusion can be reached. As in Ledford and Tawn (1996, 1997), here this is done
245 by observing the proportion of time $\eta = 1$ is within the profile likelihood confidence
246 interval for η , when estimated over a range of values of w . The pair (X, Y) are said to
247 be asymptotically dependent if $\eta = 1$ is contained within these confidence intervals for a
248 majority of the range of w , and asymptotically independent otherwise. This exploration



249 is presented for London paired with Amsterdam and Madrid in Fig. 4, confirming the
250 diagnosis of asymptotic independence for both pairs, based on this criterion. Indeed, the
251 same conclusion is reached when applying this methodology to additional pairs of land
252 locations within the European domain, including neighbouring locations.

253 **3.4 Why are wind gust speeds asymptotically independent?**

254 It is of interest to ask whether there are fundamental fluid dynamical reasons for why
255 wind gust speeds should be asymptotically independent at different spatial locations.

256 One approach to answering this question is to consider extremal dependence in tur-
257 bulent flows. The atmospheric flow in storm track regions is highly chaotic and irregular
258 and is therefore turbulent rather than smoothly varying laminar flow (see Held 1999; and
259 references therein). Furthermore, over short enough spatial distances, the horizontal flow
260 in a storm may be considered to be stationary in space and directionally invariant, in
261 other words, homogeneous isotropic turbulence.

262 As originally proposed by Von Kármán (1937), turbulent wind fields can be efficiently
263 and realistically simulated using stochastic processes (Mann, 1998). This approach is
264 widely used for many applications such as testing loads on new aircraft designs. The
265 basic assumption in homogeneous turbulence is that the Cartesian velocity components
266 are independent Gaussian processes, each with a prescribed spatial covariance function.
267 In the special case of isotropic turbulence, the spatial covariance functions are identical
268 for each velocity component. Hence, for 2-dimensional windstorm gusts, the wind gust
269 speed at spatial location, s , is given by $X(s) = \sqrt{u^2 + v^2}$, where $u = u(s)$ and $v = v(s)$
270 are independent Gaussian processes having identical covariance functions.

271 So what can be deduced about the extremal dependence class of wind speeds from



272 such turbulence models? Firstly, since the individual velocity components are bivariate
273 normal, they are asymptotically independent at different locations e.g. $u_1 = u(s_1)$ and
274 $u_2 = u(s_2)$ are asymptotically independent when s_1 differs from s_2 , and likewise for $v(s)$.
275 Furthermore, the square of each velocity component is also asymptotically independent.
276 This can be proven by noting that $\Pr(u_1^2 > t^2) = 2\Pr(u_1 > t)$ and $\Pr(u_1^2 > t^2, u_2^2 > t^2) \leq$
277 $4\chi_{max}\Pr(u_1 > t)$ where

$$\chi_{max} = \frac{\max(\Pr(u_1 > t, u_2 > t), \Pr(u_1 > t, u_2 \leq -t))}{\Pr(u_1 > t)},$$

278 and for bivariate normal velocity components $\chi_{max} \rightarrow 0$ as the threshold $t \rightarrow \infty$. The
279 squared wind speeds at pairs of locations are sums of two such independent components,
280 $(X^2, Y^2) = (u_1^2 + v_1^2, u_2^2 + v_2^2)$, and so it would be surprising if somehow this pair were not
281 also asymptotically independent.

282 Unfortunately a proof of asymptotic independence between (X^2, Y^2) (and hence (X, Y))
283 remains elusive. However, the conjecture can be tested by numerical simulation. By
284 simulating velocities from bivariate normal distributions, we have found no evidence of
285 extremal dependence in wind speeds even when each velocity component is highly cor-
286 related. Figure 5 shows an example obtained by simulating a million wind speeds at
287 two locations where the u and v velocity components are independent standard normal
288 variates each with correlation of 0.9 between locations (i.e. the correlation between u_1
289 and u_2 is 0.9). The squared wind speeds at each location are chi-squared distributed
290 with 2 degrees of freedom but are not independent: there is positive association clearly
291 visible in Fig. 5(a). To assess extremal dependence, Fig. 5(b) shows how the joint
292 exceedance probability, $\Pr(X^2 > t^2, Y^2 > t^2)$, and the marginal exceedance probability,
293 $\Pr(X^2 > t^2) = \Pr(Y^2 > t^2)$, behave as threshold t^2 is varied. As the threshold is increased

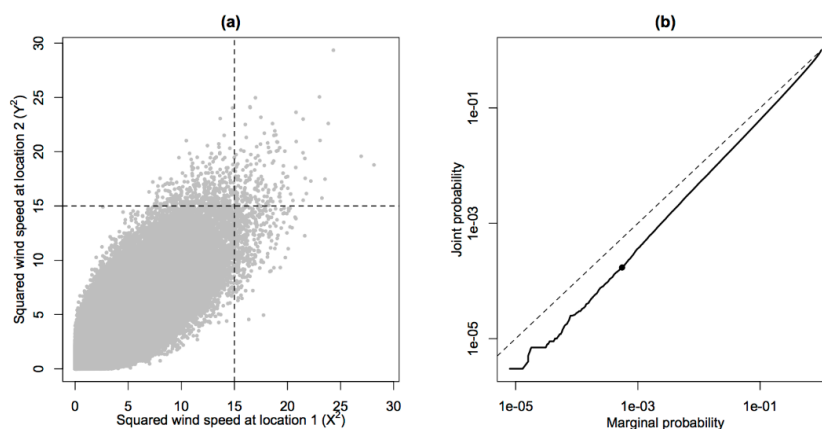


Figure 5: Simulation of wind speeds at two sites having highly correlated velocities (see main text for details): (a) scatter plot of squared wind speeds at the two sites (1000 points randomly sampled out of the million); (b) joint versus marginal exceedance probabilities (on logarithmic axes). The dot shows an example obtained by counting the fraction of points in the upper right and the right hand quadrants of (a). The curve has a steeper slope than the dashed line (equal probabilities denoting complete dependence) suggesting asymptotic independence.



294 the joint probability drops to zero faster than the marginal exceedance probability (the
295 curve in Fig. 5(b) is steeper than the dashed line), which suggests that the ratio, the
296 conditional probability of exceedance, equivalent to χ in Eqn. (1), will tend to zero in
297 the asymptotic limit.

298 4 Loss Distributions

299 To explore the importance of correctly modelled extremal dependence on the distribution
300 of a conceptual loss, we first define a conceptual loss function and then use it to compare
301 how well the Gumbel and Gaussian copula dependence models, characterising opposing
302 extremal dependence class, are able to represent empirical conceptual losses.

303 In the absence of insurance industry exposure and vulnerability information, we define
304 conceptual windstorm loss as a function of the footprint wind gust speeds, similar to
305 many examples in the literature (see Dawkins et al. (2016) for a review). Following the
306 conclusions of Roberts et al. (2014) and Dawkins et al. (2016), we propose a threshold
307 exceedance conceptual loss function over land locations in Europe. Roberts et al. (2014)
308 and Dawkins et al. (2016) showed that this form of loss function is more representative of
309 extreme windstorm loss than the commonly used, more complex loss function of Klawa
310 and Ulbrich (2003), which includes additional terms for cubed wind gust speed magnitude
311 and population density. Roberts et al. (2014) used an exceedance threshold of 25ms^{-1}
312 while Dawkins et al. (2016) used a threshold of 20ms^{-1} , in line with the loss threshold
313 used by German insurance companies (Klawa and Ulbrich, 2003). Here, however, similar
314 to Klawa and Ulbrich (2003), we propose a locally varying wind gust speed quantile
315 threshold, accounting for local adaptation to varying wind intensity.

316 Figure 6 shows that the 99% quantile of windstorm footprint wind gust speed is in

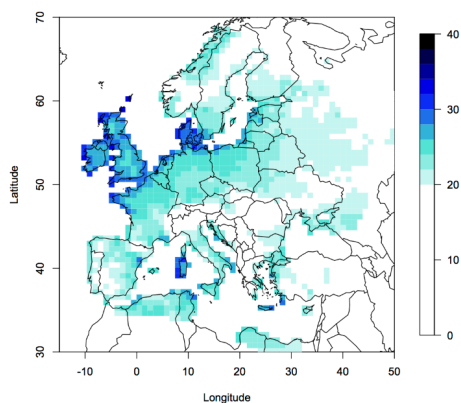


Figure 6: The 99% quantile of windstorm footprint wind gust speeds (ms^{-1}) at land locations in Europe, used as the threshold above which windstorm conceptual insured losses occur.

317 excess of the commonly used 20ms^{-1} loss threshold for most land locations in Europe,
318 with a higher loss threshold used in regions where stronger winds occur. Hence, we define
319 our bivariate conceptual loss function for the pair (X, Y) as,

$$L(X, Y) = H(X - x_{0.99}) + H(Y - y_{0.99}),$$

320 where $H(m)$ is a Heaviside function: $H(m) = 1$ if $m > 0$ and $H(m) = 0$ otherwise.
321 Hence, for a given pair of locations the conceptual loss can take the values 0, 1 or 2
322 depending on the joint exceedance of X and Y above their respective 99% quantiles, $x_{0.99}$
323 and $y_{0.99}$, equivalent to falling within the four sections in Fig. 2.

324 The probability mass function of the conceptual loss function can easily be obtained
325 by considering the joint probability of (X, Y) in each of the quadrants shown in Fig. 2:



$$\Pr(L(X, Y) = 2) = \chi(p)p,$$

$$\Pr(L(X, Y) = 1) = 2(1 - \chi(p))p,$$

$$\Pr(L(X, Y) = 0) = 1 + p(\chi(p) - 2).$$

326 From this, it is straightforward to derive the following 1st and 2nd moments:

$$\mathbb{E}(L(X, Y)) = 2\chi(p)p + 2(1 - \chi(p))p = 2p,$$

$$\mathbb{E}(L(X, Y)|L(X) = 1) = 2\chi(p)p + (1 - \chi(p))p = p(\chi(p) + 1), \quad (5)$$

$$\text{Var}(L(X, Y)) = 2(1 + \chi(p))p - 4p^2 = 2p(1 + 2\chi(p) - 2p).$$

327 Although the expected loss does not depend on $\chi(p)$, the conditional expectation and the
328 variance of loss both depend on $\chi(p)$ as well as the marginal probability of exceedance p .
329 The conditional expectation and the variance increase considerably as χ goes from 0 to
330 1.

331 We will now illustrate this by comparison of different extremal dependence class mod-
332 els. For London paired with each land location (grid cell) in Europe, we fit both the
333 Gumbel and Gaussian copula dependence models, and explore how well these two models
334 represent empirical conceptual losses. This is done in two ways.

335 Firstly by comparing the empirical, Gaussian and Gumbel estimates for $\chi(p)$ and $\bar{\chi}(p)$
336 for $p = 0.01$ (Table 1), i.e. representing measures of the conditional probability of a loss
337 occurring in Y (e.g. Amsterdam), given a loss has occurred in X (e.g. London), shown
338 in Fig. 7. Secondly, as presented in Fig. 8, by comparing the distribution, for all land
339 locations in the European domain, of the expected conditional joint loss with London,
340 given a loss has occurred in London (Eqn. 5), again calculated empirically and using the

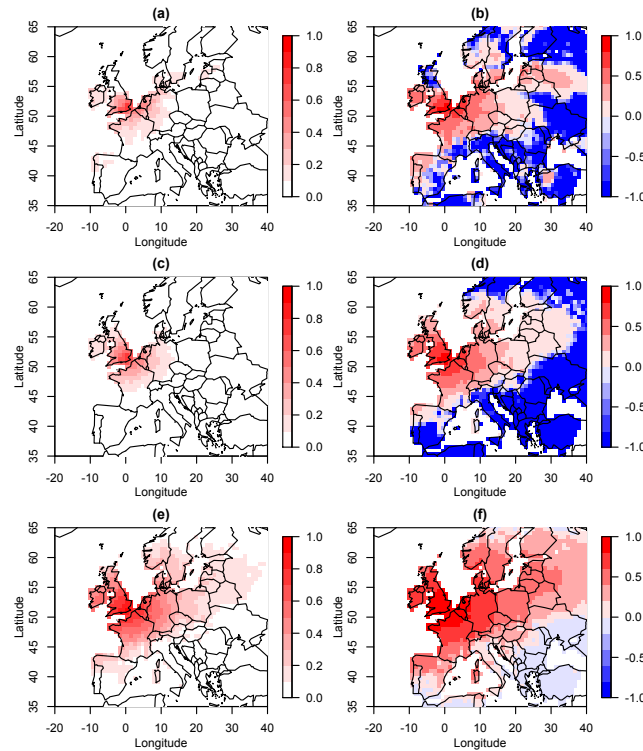


Figure 7: (a)/(b) Empirical, (c)/(d) Gaussian, and (e)/(f) Gumbel estimates of $\chi(0.01)/\bar{\chi}(0.01)$, representing measures of the conditional probability of a conceptual loss occurring at each land location in the European domain, given a conceptual loss has occurred in London.

341 two apposing dependence models.

342 Figure 7 identifies a large over estimation in both $\chi(0.01)$ and $\bar{\chi}(0.01)$ for the Gumbel
343 dependence model, when compared with the empirical estimates, due to a misspecifica-
344 tion of asymptotic dependence between locations. The Gaussian model, on the other
345 hand, which correctly represents the identified asymptotic independence between loca-
346 tions, provides a good representation of the empirical conditional loss measures, with
347 the spatial range of $\chi(0.01) > 0$ and areas of positive and negative $\bar{\chi}(0.01)$ in general

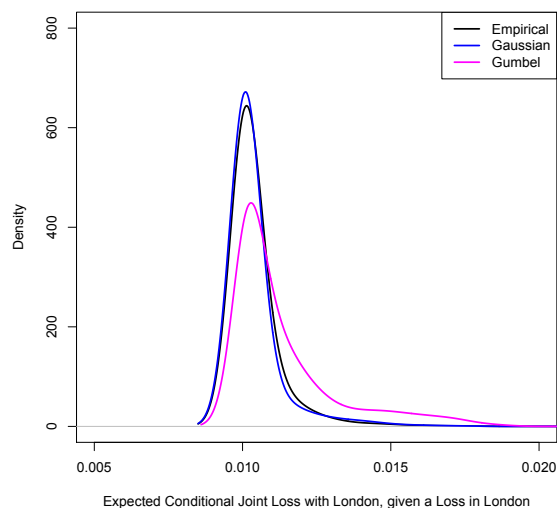


Figure 8: For all land locations in the European domain, the expected conditional joint loss with London, given a loss has occurred in London (Eqn. 5), calculated empirically and using the Gaussian and Gumbel copula models.

348 agreement with the empirical values.

349 Figure 8, further illustrate the importance of correctly specifying extremal dependence
350 class when representing loss. When a conceptual loss occurs in London, the Gumbel
351 dependence model over estimates the expected conditional joint loss with other European
352 land locations, while conversely, the Gaussian model provides a very good estimate of the
353 empirical expected conditional joint loss distribution.

354 5 Conclusion

355 This study has shown how to explore and identify extremal dependence in hazard fields
356 using extremal dependence coefficients, $\chi(p)$ and $\bar{\chi}(p)$, and estimates of the tail depen-



357 dence parameter Ledford and Tawn (1996). These measures have been compared to what
358 one would expect from Gaussian and Gumbel copulas.

359 These methods have revealed strong evidence of asymptotic independence in wind-
360 storm footprint hazard fields, contrary to what has been assumed in previous studies
361 such as Bonazzi et al. (2012). A reason for this lack of asymptotic dependency has been
362 proposed based on arguments from turbulence theory. It is shown that mis-specification
363 of the dependency (e.g. by using a Gumbel copula) leads to severe over-estimation of the
364 probability of joint losses.

365 These results provide justification that spatial representation and simulation of wind-
366 storm hazard fields can be represented by a Gaussian geostatistical model, such as that
367 developed in Chapter 5 of Dawkins (2016), rather than a max-stable, asymptotically
368 dependent model.

369 Acknowledgements

370 Laura C. Dawkins was supported by the Natural Environment Research Council (Con-
371 sortium on Risk in the Environment: Diagnostics, Integration, Benchmarking, Learning
372 and Elicitation (CREDIBLE project); NE/J017043/1).

373 References

374 Blanchet, J., Marty, C., and Lehning, M. (2009). Extreme value statistics of snowfall in
375 the Swiss Alpine region. *Water Resources Research*, 45.

376 Bonazzi, A., Cusack, S., Mitás, C., and Jewson, S. (2012). The spatial structure of Eu-



- 377 ropean wind storms as characterized by bivariate extreme-value copulas. *Nat. Hazards*
378 *Earth Syst. Sci.*, 12:1769–1782.
- 379 Bortot, P., Coles, S., and Tawn, J. (2000). The multivariate gaussian tail model: an
380 application to oceanographic data. *Applied Statistics*, 49:31–49.
- 381 Coles, S., Heffernan, J., and Tawn, J. (1999). Dependence measures for extreme value
382 analysis. *Extremes*, 2(4):339–365.
- 383 Coles, S. G. and Walshaw, D. (1994). Directional modelling of extreme wind speeds.
384 *Journal of the Royal Statistical Society. Series C (Applied Statistics)*, 43(1):139–157.
- 385 Dawkins, L. C. (2016). *Statistical modelling of European windstorm footprints to explore*
386 *hazard characteristics and insured loss*. PhD thesis, University of Exeter, College of
387 Engineering Mathematics and Physical Sciences.
- 388 Dawkins, L. C., Stephenson, D. B., Lockwood, J. F., and Maisey, P. E. (2016). The 21st
389 century decline in damaging european windstorms. *Natural Hazards and Earth System*
390 *Science*, 16:1999–2007.
- 391 Dee, D., Uppala, S. M., Simmons, A. J., Berrisford, P., Poli, P., Kobayashi, S., Andrae,
392 U., Balmaseda, M. A., Balsamo, G., Bauer, P., Bechtold, P., Beljaars, A. C. M., van de
393 Berg, L., Bidlot, J., Bormann, N., Delsol, C., Dragani, R., Fuentes, M., Geer, A. J.,
394 Haimberger, L., Healy, S. B., Hersbach, H., Hólm, E. V., Isaksen, L., Kallberg, P.,
395 Kohler, M., Matricardi, M., McNally, A. P., Monge-Sanz, B. N., Morcrette, J. J., Park,
396 B. K., Peubey, C., de Rosnay, P., Tavolato, C., Thepaut, J. N., and Vitart, F. (2011).
397 The ERA interim reanalysis: configuration and performance of the data assimilation
398 system. *Quart. J. Roy. Meteorol. Soc.*, 137:553–597.



- 399 Eastoe, E. F., Koukoulas, S., and Jonathan, P. (2013). Statistical measures of extremal
400 dependence illustrated using measured sea surface elevations from a neighbourhood of
401 coastal locations. *Ocean Engineering*, 62:68–77.
- 402 Ferro, C. A. T. (2007). A probability model for verifying deterministic forecasts of
403 extreme events. *Weather Forecasting*, 22:1089–1100.
- 404 Haylock, M. (2011). European extra-tropical storm damage risk from a multi-model
405 ensemble of dynamically-downscaled global climate models. *Natural Hazards and Earth
406 System Science*, 11:2847–2857.
- 407 Held, I. M. (1999). The macroturbulence of the troposphere. *Tellus A: Dynamic Meteo-
408 rology and Oceanography*, 51A-B:59–70.
- 409 Hodges, K. I. (1995). Feature tracking on the unit sphere. *Monthly Weather Review*,
410 123:3458–3465.
- 411 Huser, R. and Davison, A. C. (2013). Space–time modelling of extreme events. *Journal
412 of the Royal Statistical Society: Series B (Methodology)*, 76(2):439–461.
- 413 Klawa, M. and Ulbrich, U. (2003). A model for the estimation of storm losses and the
414 identification of severe winter storms in Germany. *Natural Hazards and Earth System
415 Sciences*, 3:725–732.
- 416 Ledford, A. W. and Tawn, J. A. (1996). Statistics for near independence in multivariate
417 extreme values. *Biometrika*, 83(1):169–187.
- 418 Ledford, A. W. and Tawn, J. A. (1997). Modelling dependence within joint tail regions.
419 *Journal of the Royal Statistical Society*, 59(2):475–499.



420 Mann, J. (1998). Wind field simulation. *Probabilistic engineering mechanics*, 13(4):269–
421 282.

422 Roberts, J. F., Dawkins, L., Youngman, B., Champion, A., Shaffrey, L., Thornton, H.,
423 Stevenson, D. B., Hodges, K. I., and Stringer, M. (2014). The XWS open access
424 catalogue of extreme windstorms in Europe from 1979 to 2012. *Natural Hazards and*
425 *Earth System Science*, 14:2487–2501.

426 Von Kármán, T. (1937). The fundamentals of the statistical theory of turbulence. *Journal*
427 *of the Aeronautical Sciences*, 4(4):131–138.

428 Wadsworth, J. L., Tawn, J. A., Davison, A. C., and Elton, D. M. (2017). Modelling
429 across extremal dependence classes. *Journal of the Royal Statistical Society: Series B*
430 *(Methodology)*, 79(1):149–175.

431 Youngman, B. D. and Stephenson, D. B. (2016). A geostatistical extreme-value frame-
432 work for fast simulation of natural hazard events. *Proceedings of the Royal Society A*,
433 472(20150855).



Table 1: Empirical and Parametric forms for extremal dependence measures $\chi(p)$ and $\bar{\chi}(p)$.

	$\chi(p)$	$\bar{\chi}(p)$
Empirical	$\frac{a}{a+c}$	$\frac{2 \log(a+c)/n}{\log(a/n)} - 1$
Power Law	$\frac{1}{n} \exp\left(\frac{\alpha}{\eta}\right) p^{\frac{1}{\eta}-1}$	$\frac{2 \log(p)}{\log\left(\frac{1}{n} \exp\left(\frac{\alpha}{\eta}\right)\right) + \frac{1}{\eta} \log(p)} - 1$
Gumbel	$\sim 2 - \frac{(2 \log(1-p))^{\frac{1}{r}}}{\log(1-p)} = 2 - 2^{\frac{1}{r}}$ (Coles et al., 1999)	$\frac{2 \log(p)}{\log(2p(1-p)^2)} - 1$
Gaussian	$\bar{F}(1-p, 1-p)/p,$ where $\bar{F}(1-p, 1-p) = Pr(X > x_{1-p}, Y > y_{1-p}) \sim (1+\rho)^{\frac{3}{2}}(1-\rho)^{\frac{1}{2}}(4\pi)^{-\frac{\rho}{1+\rho}}(-\log(p))^{\frac{\rho}{1+\rho}}p^{\frac{2}{1+\rho}}$ as $p \rightarrow 0$ (Coles et al., 1999)	$\frac{2 \log(p)}{\log(\bar{F}(1-p, 1-p))} - 1$